International Conference on Nuclear Data for Science and Technology 2007
DOI: 10.1051/ndata:07607

Deformation dependent TUL multi-step direct model

H. Wienke[1,a], R. Capote[2], M. Herman[3], and M. Sin[4]

[1] Belgonucleaire, 2480 Dessel, Belgium
[2] International Atomic Energy Agency, Nuclear Data Section, 1400 Vienna, Austria
[3] National Nuclear Data Center, BNL, Upton, NY 11973, USA
[4] Nuclear Physics Department, University of Bucharest, P.O. Box MG-11, Bucharest-Magurele, Romania

Abstract. The Multi-Step Direct (MSD) module TRISTAN in the nuclear reaction code EMPIRE has been extended to account for nuclear deformation. The new formalism was tested in calculations of neutron emission spectra emitted from the ^{232}Th(n,xn) reaction. These calculations include vibration-rotational Coupled Channels (CC) for the inelastic scattering to low-lying collective levels, "deformed" MSD with quadrupole deformation for inelastic scattering to the continuum, Multi-Step Compound (MSC) and Hauser-Feshbach with advanced treatment of the fission channel. Prompt fission neutrons were also calculated. The comparison with experimental data shows clear improvement over the "spherical" MSD calculations and JEFF-3.1 and JENDL-3.3 evaluations.

1 Introduction

In the nuclear reaction code EMPIRE [1] the approach to direct inelastic scattering to the continuum, as incorporated in the modules TRISTAN and ORION, is based upon the MSD quantum theory of pre-equilibrium processes originally formulated by Tamura, Udagawa and Lenske [3] (TUL) and extended with respect to statistical and dynamic treatment of nuclear structure [4]. The ORION module calculates one- and two-step cross sections with average state-independent form-factors. These one- and two-step cross sections are folded with the nuclear spectroscopic strength functions, derived in the TRISTAN module, which specify the microscopic nuclear structure properties within the framework of the Random Phase Approximation (RPA). In the currently distributed 2.19 version of the EMPIRE [1,2] code, the spectroscopic strength functions are derived assuming the scattering nucleus to be spherical. This approach well predicts double-differential neutron emission spectra (DDNES) from quasi-spherical ^{93}Nb nucleus induced by 14.1 MeV neutrons (see, *e.g.*, EMPIRE-2.19 manual [1], p. 158). However, similar emission spectra from the deformed nucleus ^{232}Th induced by $E_{inc} \geq 6.1$ MeV neutrons are severely under predicted in the region of direct inelastic scattering to the continuum. To address this deficiency, the TRISTAN module has been modified to account for nuclear deformation, and incorporated into the EMPIRE-2.19beta35 code which has been applied in calculations of DDNES from the n+^{232}Th reaction. The updated formalism, which underlies the modifications in TRISTAN, is outlined. Computed results are compared with experimental data [5–7] and existing evaluations.

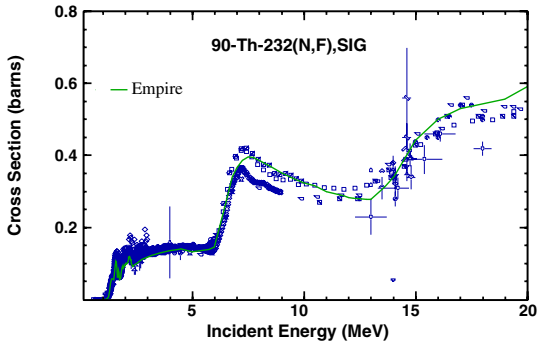

Fig. 1. ^{232}Th(n,fission) cross section.

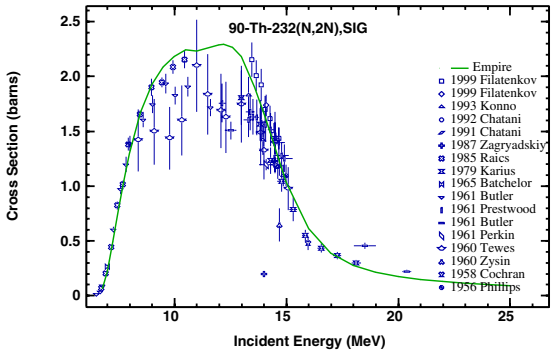

Fig. 2. ^{232}Th(n,2n) cross section.

2 Updated formalism in TRISTAN

In the current official version of the TRISTAN module, nuclear single-particle energies and wave functions are obtained from a spherical Nilsson Hamiltonian with standard parameters. Pairing correlations are accounted for by the BCS method in the constant gap approximation. The resulting two-quasi-particle (2qp) excitation energies and wave functions determine the uncorrelated 2qp multipole nuclear Green functions $G_L^{2qp}(\varepsilon)$. The uncorrelated $2qp$ response function for an external one-body multipole field $U_L = v(r)Y_L$ is then $\chi_L^{2qp}(\varepsilon) = \langle c|\, U_L^\dagger\, G_L^{2qp}(\varepsilon)\, U_L|c\rangle$, $|c\rangle$ being an initial reference state. In the RPA schematic model, a separable residual particle-hole interaction of the form $V^{sep}(1,2) = \sum_L \kappa_L U_L(1) U_L(2)$ is assumed. Then the quasi-particle RPA (QRPA) correlated

[a] Presenting author, e-mail: h.wienke@belgacom.net

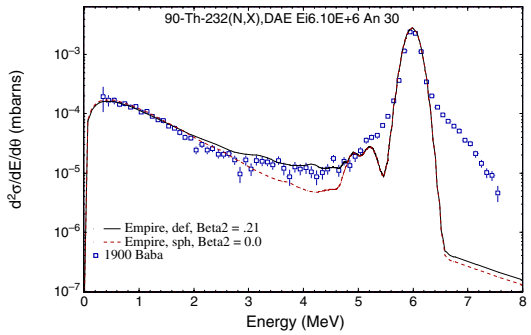

Fig. 3. ^{232}Th(n,xn) DDNES, deformed + spherical MSD, E_{inc} = 6.1 MeV, 30 deg.

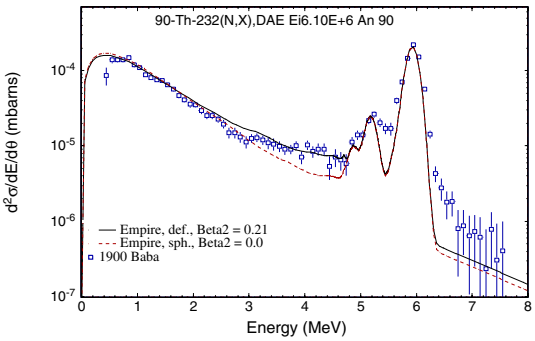

Fig. 4. ^{232}Th(n,xn) DDNES, deformed + spherical MSD, E_{inc} = 6.1 MeV, 90 deg.

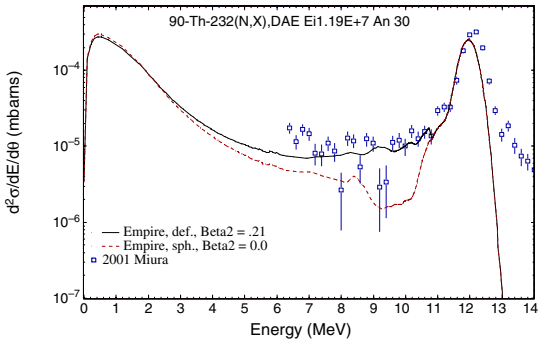

Fig. 5. ^{232}Th(n,xn) DDNES, deformed + spherical MSD, E_{inc} = 11.9 MeV, 30 deg.

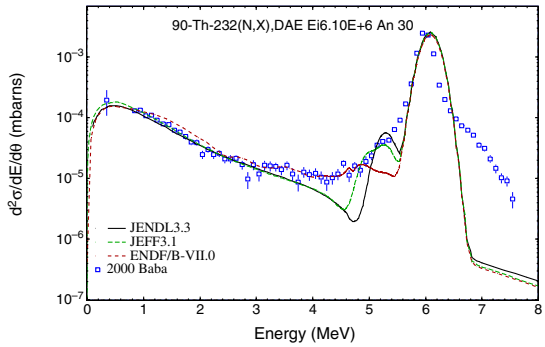

Fig. 6. ^{232}Th(n,xn) DDNES, E_{inc} = 6.1 MeV, 30 deg, ENDF-B7.0, JEFF-3.1 and JENDL-3.3 data.

response function for the operator U_L is obtained from the Bethe-Salpeter (B-S) equation [8]

$$\chi_L^{QRPA}(\varepsilon) = \chi_L^{2qp}(\varepsilon) + \kappa_L \chi(_L^{2qp}(\varepsilon)\chi_L^{QRPA}(\varepsilon)\,. \qquad (1)$$

The multipole spectroscopic strength function of multipolarity L is $S_L(\varepsilon) = -Im\chi_L^{QRPA}(\varepsilon + i\Gamma/2)/\pi$, Γ being the spreading width [1]. In the extended version of the TRISTAN module, a quadrupole deformation term has been added to the nuclear Hamiltonian. The quadrupole deformation value is taken from the EMPIRE input. As the nuclear Hamiltonian is now non-diagonal in the spherical Nilsson basis, the $2qp$ wave functions are, in contrast with the degenerate case, not eigenfunctions of the squared angular momentum L^2. Consequently the uncorrelated $2qp$ multipole nuclear Green functions are not diagonal with respect to L. However, because of the symmetry with respect to the deformation axis, both parity π and angular momentum projection K onto this axis are still conserved. The uncorrelated $2qp$ multipole response function for the external one-body field $U_{L,K} = v_{L,K}(r)Y_L^K$ then becomes

$$\begin{aligned}\chi_{L,K}^{2qp}(\varepsilon) &= \langle c| \sum_{L'} U_{L,K}^{\dagger}\, G_{L,L',K}^{2qp}(\varepsilon)\, U_{L,K}\, |c\rangle \\ &= \langle c|\, U_{L,K}^{\dagger}\, G_{L,L,K}^{2qp}(\varepsilon)\, U_{L,K}\, |c\rangle\,. \end{aligned} \qquad (2)$$

The QRPA correlated response function is obtained in the schematic RPA from the B-S equation for each K [9]

$$\begin{aligned}\chi_{L,K}^{QRPA}(\varepsilon) &= \chi_{L,K}^{2qp}(\varepsilon) + \kappa_{L,K}\chi_{L,K}^{2qp}(\varepsilon)\,\chi_{L,K}^{QRPA}(\varepsilon) \\ &\quad + [\text{off-diagonal terms in } L]\,. \end{aligned} \qquad (3)$$

The calculation of the multipole spectroscopic strength function S_L now involves a summation over K of $Im\chi_{L,K}^{QRPA}$. it can be shown that the contributions of the off-diagonal terms in the B-S equation to the spectroscopic strength function are neglibly small compared to the diagonal terms [14].

3 EMPIRE calculations

The updated formalism, as implemented in the EMPIRE-2.19beta35 code, has been applied in calculations of DDNES from n+^{232}Th above 4.5 MeV, where MSD contribution is sizeable. MSD inelastic neutron scattering to the continuum ($E_{ex} \geq 1.19$ MeV) was calculated using a quadrupole deformation $\beta_2 = 0.21$. The inelastic-scattering cross sections to excited levels in the discrete region ($E_{ex} < 1.19$ MeV) and the neutron transmission coefficients for the neutron channel were obtained with the coupled-channel code ECIS03 [10] incorporated in Empire-2.19. The dispersive coupled-channel optical model potential of Soukhovitskii et al. [11] was used as quoted in the RIPL library (RIPL 605) [12]. Nineteen levels, five from the ground-state rotational band and the few lowest from the $K^\pi = 0^+$(730.5 keV) β-vibration, $K^\pi = 2^+$(785.5 keV) γ-vibration and $K^\pi = 0^+$(1078.7 keV) anomalous quadrupole vibrational bands as well as the $K^\pi = 0^-$(714.25 keV) octupole vibrational band [13], were coupled simultaneously within the vibration-rotational model [14]. It was found that inclusion of additional members of the above bands in the coupling does not change the results of calculations noticeably in comparison with the original coupling scheme [11]. The

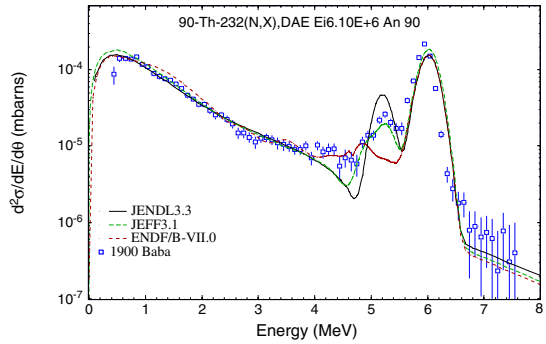

Fig. 7. ^{232}Th(n,xn) DDNES, E_{inc} = 6.1 MeV, 90 deg, ENDF-B7.0, JEFF-3.1 and JENDL-3.3 data.

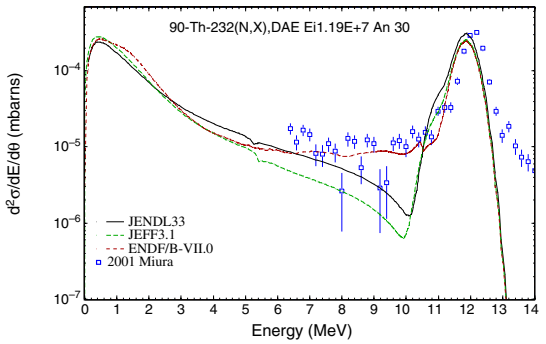

Fig. 8. ^{232}Th(n,xn) DDNES, E_{inc} = 11.9 MeV, 30 deg, ENDF-B7.0, JEFF-3.1 and JENDL-3.3 data.

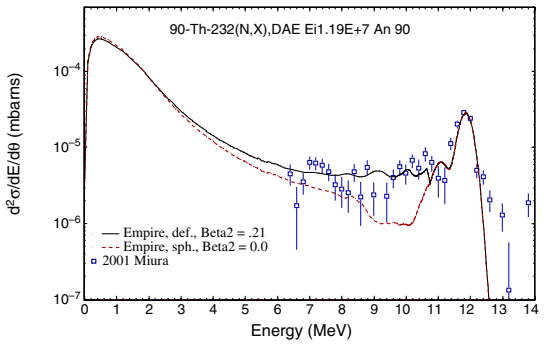

Fig. 9. ^{232}Th(n,xn) DDNES, deformed + spherical MSD, E_{inc} = 11.9 MeV, 90 deg.

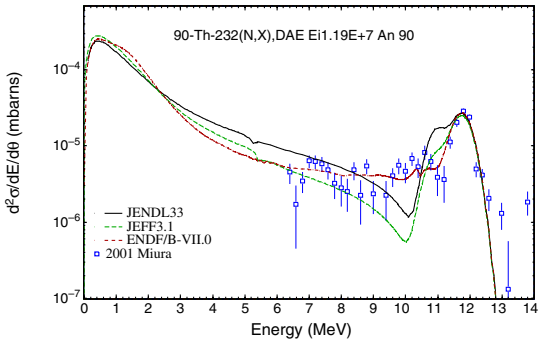

Fig. 10. ^{232}Th(n,xn) DDNES, E_{inc} = 11.9 MeV, 90 deg, ENDF-B7.0, JEFF-3.1 and JENDL-3.3 data.

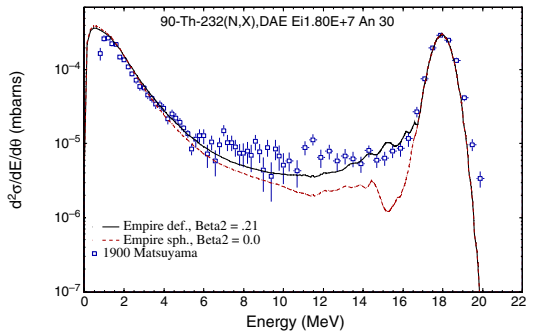

Fig. 11. ^{232}Th(n,xn) DDNES, deformed + spherical MSD, E_{inc} = 18 MeV, 30 deg.

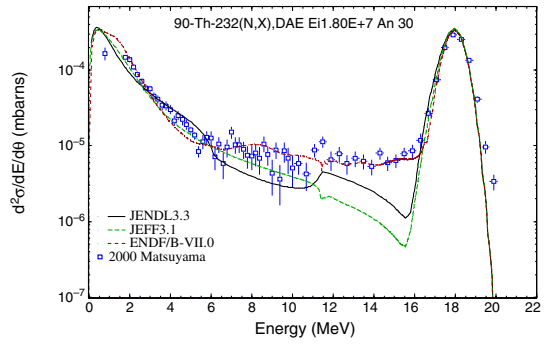

Fig. 12. ^{232}Th(n,xn) DDNES, E_{inc} = 18 MeV, 30 deg, ENDF-B7.0, JEFF-3.1 and JENDL-3.3 data.

dynamical deformations of the phonons involved were taken from literature or obtained by adjustment to the data. Pre-equilibrium compound neutron emission was calculated in the Heidelberg multi-step compound (MSC) approach [15]. The total neutron emission spectra was obtained as a incoherent sum of both MSD and MSC contributions. Equilibrium compound decay was treated within the Hauser Feshbach statistical model [16] with decay probabilities obtained in the optical model for fission [17]. The resulting neutron emission spectra also include prompt fission neutrons [18].

4 Results and discussion

The calculated cross sections versus incident neutron energy of the competing ^{232}Th(n,2n) and ^{232}Th(n,f) processes nicely agree with the experimental data (see fig. 1 and 2). Figures 3, 4, 5, 9, 11 present the EMPIRE-2.19 calculations of the DDNES from the ^{232}Th(n,xn) reaction, with and without consideration of the nuclear quadrupole deformation, together with the experimental data for selected emission angles at incident neutron energies 6.1 [5], 11.9 [6] and 18 MeV [7], respectively. The EMPIRE-2.19 calculations accounting for nuclear deformation in MSD nicely reproduce the data in the direct continuum region ($\sim 5 \geq E_{ex} \geq 1.19$ MeV) while the "spherical" calculations underpredict the same data by a factor ~3 at 6.1 MeV, up to a factor ~8 at 18 MeV. Figures 6, 7, 8, 10, 12 show the corresponding DDNES from the JENDL-3.2 and JEFF-3.1 evaluations and the recent IAEA evaluation

[18] adopted for the ENDF/B-VII.0 library. The "deformed" EMPIRE results show overall better agreement with the measurements than the corresponding JENDL-3.2 and JEFF-3.1 evaluations and similar agreement as the IAEA evaluation. It should be stressed that, except for adjustment of dynamic deformations used in the coupled-channel calculations and the fission input taken over from the previous exercise [17], present results were obtained without any additional parameter fitting, i.e., there was no adjustment of the MSD part of the calculations, the part that forms the essence of this paper. In the IAEA evaluation for ^{232}Th, the missing strength in the continuum region of the neutron spectrum was filled up with DWBA to a large number of fictitious collective levels embedded in the continuum. Similar approach has also been used in other ENDF/B-VII evaluations for important actinides, such as ^{235,238}U and ^{239}Pu [19]. Subsequent validation proved that the thus obtained improvements of inelastic scattering data largely improved library performance in integral benchmarking [20]. Our "deformed" MSD approach allows to achieve similar result on a physically sound basis. The method is computationally faster and has been implemented as a default in the recent (to be released) version of the EMPIRE code.

5 Conclusions

The Multi-Step Direct module TRISTAN in the nuclear reaction code EMPIRE has been extended to account for nuclear quadrupole deformation of the target nucleus. The new formalism results in a substantial improvement of agreement of the DDNES from the ^{232}Th(n,xn) with experimental data in the MSD dominated range, also in comparison with corresponding JENDL-3.2 and JEFF-3.1 evaluations, and in similar agreement with measurements as the latest IAEA evaluation. This improvement is attained by advancing physical contents of the model rather than by forcing parameter values or patching the model.

References

1. M. Herman, P. Obložinský, R. Capote et al., AIP Conf. Proc. **769** (2005), p. 1184. Code distributed online at http://www.nndc.bnl.gov/empire219.
2. M. Sin, R. Capote, M. Herman et al., AIP Conf. Proc. **769** (2005), p. 1249.
3. T. Tamura, T. Udagawa, H. Lenske, Phys. Rev. C **26**, 379 (1982).
4. H. Lenske, H. Wolter, Nucl. Phys. A **358**, 483 (1992); Nucl. Phys. A **690**, 267 (2001).
5. M. Baba, H. Wakabayashi, N. Itoh et al., JAERI-M-89-143 (1989), p. 143.
6. T. Miura, M. Baba, M. Ibaraki et al., Ann. Nucl. Energy **28**, 937 (2001).
7. S. Matsuyama, M. Baba, T. Ito et al., JAERI-M-91-032 (1990), p. 219.
8. A.L. Fetter, J.D. Walecka, in *Quantum Theory of Many Body Systems* (McGraw-Hill, New York, 1971); W.H. Dickhoff, D. van Neck, in *Propagator Description of Quantum Mechanics in Many-Body Systems* (World Scientific, 2005).
9. K. Hagino, N. Van Giai, H. Sagawa, Nucl. Phys. A **731**, 272 (2004).
10. J. Raynal, Program ECIS03, OECD NEA Data bank, Paris, NEA-0850 (2004).
11. E.Sh. Soukhovitskiĭ, R. Capote, J.M. Quesada, S. Chiba, Phys. Rev. C **72**, 024604 (2005).
12. T. Belgya, O. Bersillon, R. Capote et al., IAEA-TECDOC-506, (IAEA, Vienna, 2006).
13. V.M. Maslov, INDC(BLR)-016 (IAEA, Vienna, 2003).
14. H. Wienke, M. Herman, R. Capote, M. Sin (to be published).
15. M. Herman, G. Reffo, H.A. Weidenmuller, Nucl. Phys. A **553**, 124 (1992).
16. W. Hauser, H. Feshbach, Phys. Rev. **87**, 366 (1952).
17. M. Sin, R. Capote, A. Ventura et al., Phys. Rev. C **74**, 014608 (2006).
18. R. Capote, M. Sin, A. Trkov (to be published).
19. M.B. Chadwick, P. Obložinský, M. Herman et al., Nucl. Data Sheets **107**, 2931 (2006).
20. S.C. van der Marck, Nucl. Data Sheets **107**, 3061 (2006).